Cenozoic tectonics and evolution of the Euphrates valley in Syria

V. G. Trifonov, D. M. Bachmanov, O. Ali, A. E. Dodonov, T. P. Ivanova, A. A. Syas'ko, A. V. Kachaev, N. N. Grib, V. S. Imaev, M. Ali and A. M. Al-Kafri

Geological Society, London, Special Publications v.372, first published September 6, 2012; doi 10.1144/SP372.4

Geological Society, London, Special Publications published online September 6, 2012 as doi: 10.1144/SP372.4

Cenozoic tectonics and evolution of the Euphrates valley in Syria

V. G. TRIFONOV[1]*, D. M. BACHMANOV[1], O. ALI[2], A. E. DODONOV[1], T. P. IVANOVA[3], A. A. SYAS'KO[4], A. V. KACHAEV[4], N. N. GRIB[4], V. S. IMAEV[5], M. ALI[2] & A. M. AL-KAFRI[2]

[1]*Geological Institute of the Russian Academy of Sciences (RAS), 7 Pyzhevsky, Moscow 119017, Russia*

[2]*General Organization of Remote Sensing, PO Box 12586, Damascus, Syria*

[3]*Institute of Dynamics of Geospheres of the RAS, Block 6, 38 Leninsky Ave., Moscow 117334, Russia*

[4]*Technical Institute (Branch of the Yakutsk State University), Neryungri, Russia*

[5]*Institute of the Earth's Crust of the Siberian Branch of the RAS, 128 Lermontov street, Irkutsk 664033, Russia*

**Corresponding author (e-mail: trifonov@ginras.ru)*

Abstract: Late Cenozoic tectonics affected the evolution of the Euphrates river valley in northern Syria. Data on the height and composition of terraces and new K–Ar dating of overlying basalts are presented for the area between the Assad Reservoir and the town of Abou Kamal. The presence of the Late Cenozoic Euphrates Fault, longitudinal with respect to the valley, is established by the lower height of the terraces on the NE side of the valley compared with the same terraces on the SW side. Geophysical profiling (dipole axial sounding; correlation refraction method and georadar) across the southern side of the valley (opposite the town of Ar Raqqa) confirms the offset on the fault as >25 m. Movements along the transverse Rasafeh–El Faid fault zone and the Halabiyeh–Zalabiyeh deformation zone have resulted in local uplift and the splitting of river terraces. During the Pliocene–Early Pleistocene, uplift and strong incision of the Euphrates valley propagated from near the Syrian–Turkish border to near the Iraq–Syrian border. The Euphrates began to deposit alluvium onto the pre-existing low-lying Mesopotamian Foredeep at *c.* 3.5 Ma. Intense incision began by late Late-Pliocene time to form terrace IV. Comparable incision further downstream began during the Early Pleistocene to form terrace III.

The aim of this paper is to estimate the role of Late Cenozoic tectonics on the formation and evolution of the Euphrates River valley. It will be shown that the longitudinal Euphrates Fault and associated transverse faults and related zones of deformation have influenced the Pliocene–Quaternary development of the river valley and also controlled the location and structural features of segments of the valley, specifically between the Assad Reservoir in the west and the town of Abou Kamal in the SE near the Iraq–Syrian border. The information on the Late Cenozoic fault offsets and the related deformation was mainly obtained by study of the river terraces and their Pliocene–Quaternary alluvial cover. Geophysical profiling across the southern side of the valley opposite the town of Ar Raqqa confirms existence of the young Euphrates Fault. The data obtained show that the Rasafeh–El Faid transverse fault zone borders the Aleppo Block of the Arabian plate to the east and SE and that the Euphrates Fault marks the southwestern boundary of the Mesopotamian Foredeep. The data support a new interpretation of the development of the Euphrates valley during Pliocene–Quaternary time.

Regional background

The Arabian plate is bordered to the west by the Dead Sea Transform (DST). The Syrian–Lebanon part of the DST originated at 3.4–4 Ma, when new segments formed, namely the Yammuneh Fault in Lebanon and the El Ghab Fault in Syria (Trifonov *et al.* 1991; Barazangi *et al.* 1993; Rukieh *et al.* 2005). Westaway *et al.* (2006) dates this reorganization at *c.* 3.7 Ma. The East Anatolian fault zone (EAFZ) originated along the northwestern margin of the plate at around the same time (Rukieh *et al.* 2005), or at the end of the Miocene (Westaway 2004). The northern margin of the plate is deformed

From: Robertson, A. H. F., Parlak, O. & Ünlügenç, U. C. (eds) 2012. *Geological Development of Anatolia and the Easternmost Mediterranean Region*. Geological Society, London, Special Publications, **372**, http://dx.doi.org/10.1144/SP372.4

Geological Society, London, Special Publications published online September 6, 2012 as doi:
10.1144/SP372.4

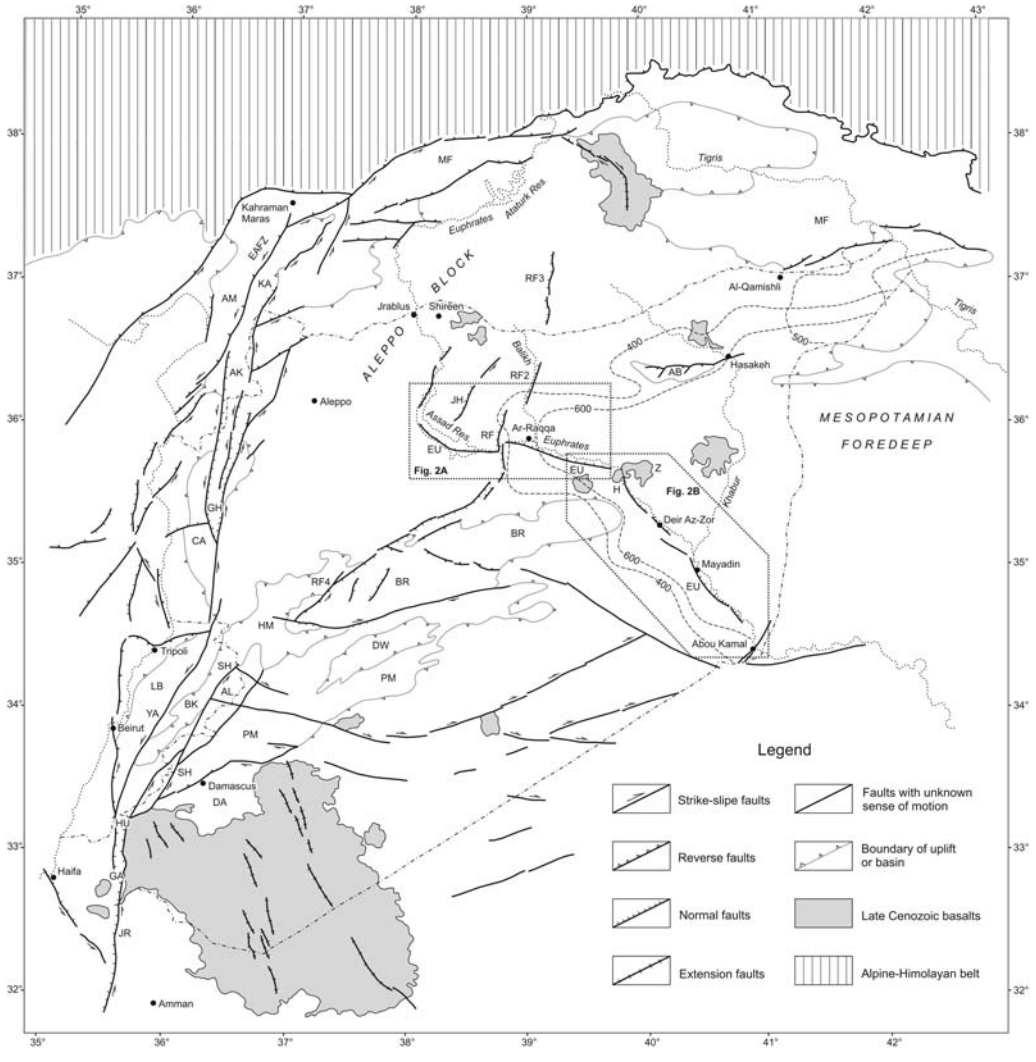

Fig. 1. Late Pliocene–Quaternary (last *c.* 3.5 Ma) tectonic features of the northern part of the Arabian plate. The 400 and 600 m Miocene isopachs and the 500 m Pliocene isopach demonstrate the structure of the Mesopotamian Foredeep. Contours of Figures 2a and b are shown. *Uplifted anticline* zones: AB, Abdel Aziz; AL, Antilebanon; BR, Bishri, the Northern Palmyrides; CA, Coastal of Syria; LB, Lebanon; MF, Marginal Folds of Turkey; PM, Southern Palmyrides. *Faults and fault zones*: AM, Amanos, a segment of the EAFZ; EAFZ, East Anatolian; EU, Euphrates; JH, Beer Jabel–Heimer Kabir; JR, Jordanian, a segment of the DST; RF, Rasafeh–Faid and its continuation (RF2, RF3 and RF4); SH, Serghaya; YA, Yammuneh, a segment of the DST. *Basins*: AK, Amik; BK, Bekkaa syncline; DA, Damascus; DW, Ad Daw; GA, Galilee Sea pull-apart basin of the Dead Sea Transform (DST); GH, El Ghab pull-apart basin of the DST; HM, Homs; HU, Hula pull-apart basin of the DST; KA, Karasu graben. *Basaltic fields*: H, Halabieh; Z, Zalabieh.

by the Marginal Folds of Turkey (Ilhan 1974). These are bounded to the north by the Bitlis (Eastern Taurus) thrust, corresponding to the Neo-Tethys suture (Robertson 2000; Robertson *et al.* 2004). The Marginal Folds and the suture continue to the SE corresponding to the folded and thrusted belt and the Main Thrust of Zagros (Golonka 2004). The Zagros belt represents the deformed northeastern margin of the Mesopotamian Foredeep. The folded and thrusted Palmyride belt adjoins the termination of the Foredeep in the west. The DST, the EAFZ and the Palmyrides border the platformal Aleppo Block (Fig. 1).

The source of the Euphrates River is situated within the Armenian Highland. In its upper reaches, the river crosses the Pontian zone of the

Alpine–Himalayan orogenic belt, the North Anatolian fault zone, the eastern Anatolian plate, the EAFZ and the Marginal Folds of Turkey. In Syria, the Euphrates valley cuts the Arabian plate (Fig. 1). From the Syrian–Turkish boundary as far as up to the Assad Reservoir, the southward trend of the valley generally parallels the eastern margin of the Aleppo Block. In the Assad Reservoir area, the river turns to the ESE and follows the southern side of the Mesopotamian Basin. The direction of the valley changes from the ESE to the SE in the Palmyrides, within the Halabiyeh and Zalabiyeh basaltic fields. Beyond this, within Iraq, the Euphrates follows the Mesopotamian Foredeep to the Persian Gulf.

Late Cenozoic deposits and terraces of the Euphrates River

Liere (1960–1961) was the first to document the Quaternary geology, geomorphology and archaeology in the Syrian part of the Euphrates valley. Systematic studies of the Late Cenozoic deposits and the geomorphology of the valley were carried out under the framework of the geological mapping of Syria (Ponikarov 1964; Ponikarov *et al.* 1967). The Pliocene was divided into the units N_2^a and N_2^b. The lower unit N_2^a is exposed in the banks of the Euphrates from Turkey to Iraq. In contrast, the upper unit N_2^b is exposed only to the east of the Khabour River mouth. The thickest (*c.* 100 m) section of the unit N_2^a has been recognized along the left bank of the Euphrates near the Turkish boundary (Ponikarov 1964; Sheet J-37-III). This section consists of clays, marls, silts, sandstones and conglomerates. Downstream, the relative abundance of conglomerates decreases and the visible thickness of the unit does not exceed 30 m. The upper unit N_2^b, which is typically up to 35 m thick, has an erosional contact with the unit N_2^a and consists of soft conglomerates and sandstones, often showing cross bedding. Some pebbles of igneous and metamorphic rocks in both of the units were eroded and transported from the inner zones of the Alpine–Himalayan belt in Turkey.

The Quaternary of the Euphrates valley was divided by the above authors into four terraces, plus recent flood plain and channel deposits. The terraces were dated as belonging to the Early, Middle and Late Pleistocene and the Early Holocene (Q_1, Q_2, Q_3, Q_4^a). Ponikarov *et al*. (1967) dated the Pliocene–Quaternary boundary only approximately, between 1 Ma and 1.8 Ma. In this paper, we use the new stratigraphic division of the Pliocene and Quaternary, confirmed in the 33rd IGC (www.stratigrahy.org). The boundary between the Early and Late Pliocene is dated as 3.6 Ma and the Pliocene–Quaternary boundary is dated as 2.588 Ma. The Quaternary is divided into the Early Pleistocene including the Gelasian (2.588–1.806 Ma) and the Calabrian (1.806–0.781 Ma), the Middle Pleistocene (0.781–0.126 Ma), the Late Pleistocene (0.126–0.011 Ma) and the Holocene (the last 0.011 Ma). Ponikarov *et al.* (1967) defined the 60–120 m terraces as Q_1; the 20–40 metre terraces as Q_2; and the 8–20 m terraces I and II as Q_3–Q_4^a. The flood plain and channel were dated as the late Holocene (Q_4^b). Archaeological finds of Levallois type were reported from the Q_3–Q_4^a terraces, together with Acheulian type finds in the Q_2 terraces (Ponikarov *et al.* 1967).

Later, Besançon and Sanlaville (1981; see also Muhesen 1985) differentiated five terraces that were dated as Pleistocene and correlated with the global isotopic-oxygen scale MIS (Marine Isotope Stages; Copeland 2004; Sanlaville 2004). Recent channel and flood plain deposits (Qf0) were excluded.

The above stratigraphy was later found to be problematic. Sharkov *et al.* (1998; see also Trifonov *et al.* 2011) determined K–Ar ages for basalts covering the terrace QfIV near the village of Halabiyeh and also the terrace QfII in the Abou Jemaa quarry east of the village of Ayash, to the NW of the town of Deir Az-Zor (Fig. 2). The Halabiyeh basalts were dated as 2.76 ± 0.09 and 2.9 ± 0.1 Ma; also, three dates from the Abou Jemaa quarry ranged from 0.71 ± 0.08 to 0.82 ± 0.07 Ma (*c.* 0.8–0.7 Ma). Recently, K–Ar dates of 2.58 ± 0.08 Ma were obtained for the Halabiyeh basalt and 0.85 ± 0.03 Ma for the Abou Jemaa basalt (Trifonov *et al.* 2011). The second of these date seems too old, since the basalt shows a normal magnetic polarity, corresponding to the Brunhes epoch, that is, not older than 0.78 Ma.

In addition, Demir *et al.* (2007) has reported contrasting $^{40}Ar/^{39}Ar$ dates for a split sample of the Halabiyeh basalt: 2764.8 ± 29.3 and 2676.4 ± 27.2 ka. The $^{40}Ar/^{39}Ar$ dating of the Zalabiyeh–Kasra basalt, which was erupted onto the surface of the 45 m high terrace QfIII, gave an age of 2116.2 ± 38.8 ka. A graph of the percentage composition by weight of alkali metal oxides against silica confirms that samples of the Zalabiyeh–Kasra basalts from different localities in fact belong to a single eruptive phase of basanite from the same volcano (Abou Romieh *et al.* 2009). A split sample of the basalt that covers the 8 m high terrace QfI to the north of the village of Ayash gave $^{40}Ar/^{39}Ar$ dates 410.6 ± 14.6 and 389.9 ± 17.0 ka, that is, *c.* 0.4 Ma (Demir *et al.* 2007). According to Demir *et al.* (2007), the last basaltic flow covers not only the terrace QfI alluvium containing the Levallois-type artefacts, but also the 23 m-high terrace QfII alluvium that contains the Acheulian-age hand-axes. [The Acheulian is the Early Paleolithic culture and

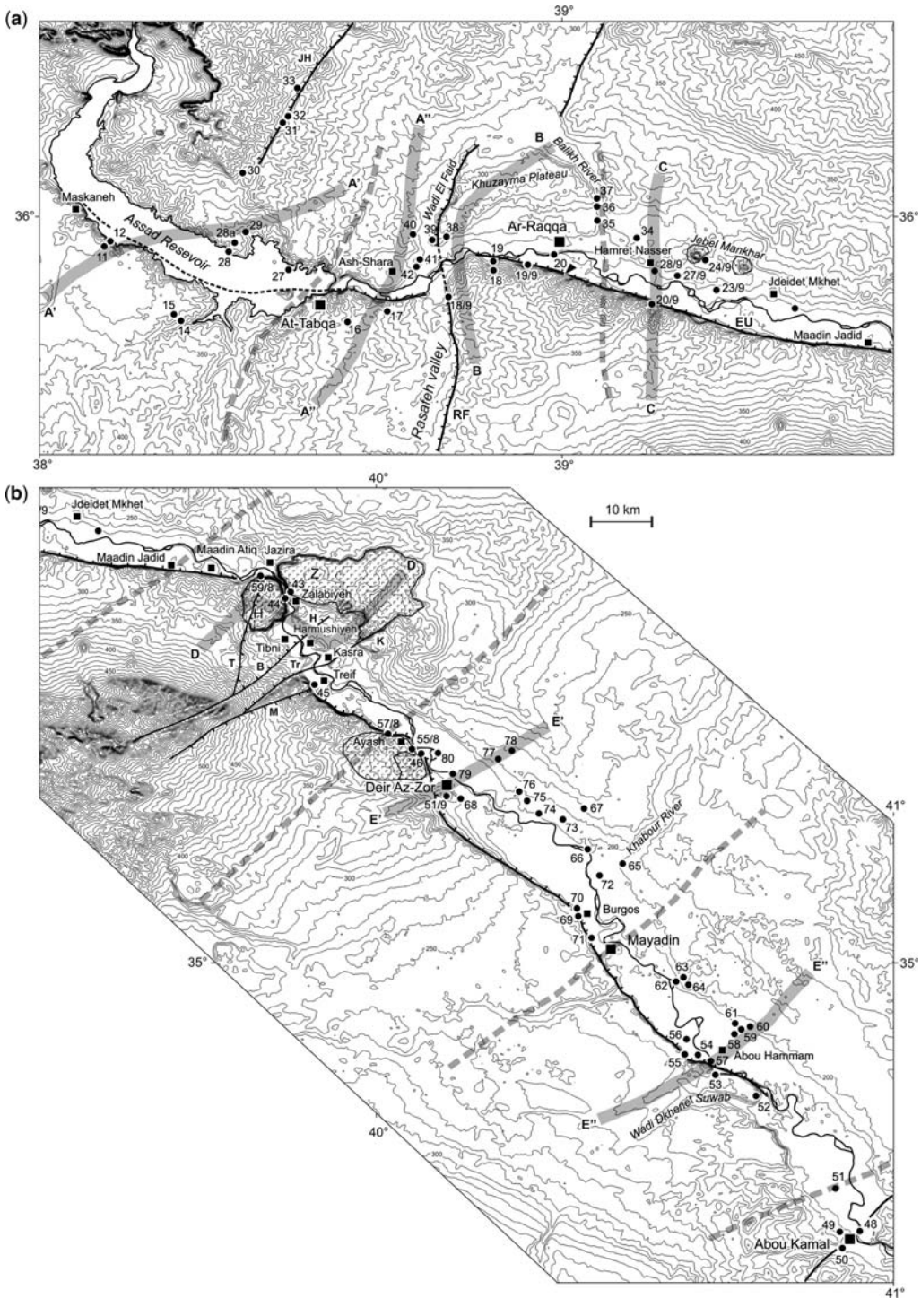

Fig. 2. The Euphrates valley between the Assad Reservoir and the town of Abou Kamal. B continues A to the SE. The map demonstrates isohypses with the 10 m interval according to the Shuttle Radar Topography Mission (SRTM) data and the location of Late Cenozoic faults, basaltic fields, sites of our observations and some trigpoints. The Euphrates

hand-axes are typical tools of the Acheulian. The Levallois technique originated in the late Acheulian, but is the most characteristic for the Middle Paleolithic (Elias 2007).] Because of this conflicting evidence we decided to re-study the area again during 2008–2010. Based on this work, the terrace QfII (*c.* 23 m high) from a quarry SE of Ayash can be described as exposing the following units from the top downwards:

(1) Basaltic flow (in places covered by up to 2 m of silt); *c.* 3 m thick; dated at *c.* 0.8–0.7 Ma.
(2) Silt with lenses of coarse material; 2–4 m thick.
(3) Fluvial conglomerates made up of several layers of rounded pebbles and boulders and also lenses of fine-grained material, exhibiting horizontal or oblique stratification, as well as sand dykes and Acheulian-type artefacts; up to 10 m thick (visible).

The *c.* 12 m high terrace QfI, as observed the northern margin of the village of Ayash (top-down) exhibits:

(1) Basaltic flow, dated by Demir *et al.* (2007) at *c.* 0.4 Ma old, covered, within a depression on the flow surface, by 1–2 m of recent silt; *c.* 3 m thick.
(2) Silt with lenses of coarser material; up to 5 m thick.
(3) Dark-grey horizontally stratified fluvial gravel with thin lenses of finer material; up to 6 m thick.

The floodplain (exposed 3–5 m above the Euphrates River) is composed of dark-grey clay and silt. Our new data and a comparison with the results of Demir *et al.* (2007) indicate that the 8–12 m high terrace QfI and the 20–23 m high terrace QfII are covered (near the village of Ayash) by basalts of different ages: that is, *c.* 0.4 and *c.* 0.7 Ma, respectively. These lavas were erupted from different volcanoes, as identified in the field and on satellite images (Trifonov *et al.* 2011). Levallois-like artefacts occur in the lower terrace sediments. Artefacts within the upper terrace alluvium are obviously older than late Acheulian.

Demir *et al.* (2007) presented data that differentiates the terrace QfIII to sublevels QfIII^{a} and QfIII^{b}. The sublevel QfIII^{b} ($\geq$45 m high) is covered by the Zalabiyeh–Kasra basalts dated as *c.* 2.12 Ma age and, thus, attributed to the Gelasian. Khattabian flake and core artefacts without hand-axes were found in alluvium of the 30–45 m-high sublevel QfIII^{a} near the villages of Maadan Jadid and Kasra in the Halabiyeh–Zalabiyeh area. The same types of artefacts have been reported in the Birecik segment of the Euphrates valley near the Syrian boundary. These artefacts were found in gravel of the *c.* 80 m high terrace, tentatively dated as *c.* 1.8–1.9 Ma (Demir *et al.* 2008). The Khattabian artefacts are assigned to the primitive Early Palaeolithic, equivalent to the Olduvan culture and, therefore, date the sublevel QfIII^{a} to the Early Calabrian.

Our revised stratigraphic scheme of the Pliocene–Quaternary terraces and deposits of the Euphrates valley is summarized in Table 1. We do not differentiate the terraces IV and V, because their height varies according to the effects of Late Cenozoic tectonics, as discussed below.

Methodology of study of the Euphrates terraces

The Euphrates River terraces include pebbles of metabasite, schist, quartzite, jasper, radiolarite, gabbroic rocks, diabase and silicic igneous rocks that were derived from the inner zones of the Alpine–Himalayan Belt in Turkey. On the other hand, lithologies including various carbonate rocks, flint and sandstones are similar to bedrock exposed within the Syrian part of the Euphrates watershed, but could also have been transported from the adjacent Turkish part of the Arabian plate. The pebbles that were transported from the inner zones of the belt are relatively rounded and are usually smaller than pebbles of local origin. This mixture of local origin and far-travelled material is here termed 'Euphrates alluvium (or gravel, or pebbles)'. Lenticular alternations of pebbles and sands represent the former channel deposits, which now make up much of the terrace deposits. In contrast, the recent flood plains are mainly made up of silts, loams and clays, 1–5 m thick, that dominate the upper part of the terrace sections. The presence of fine-grained material in the tops of the terraces indicates an absence of significant erosion.

The altitude of the individual terraces has mainly been estimated by levelling above the Euphrates River using a hand-held instrument. Possible errors

Fig. 2. (*Continued*) (EU), Rasafeh–El Faid (RF) and Beer Jabel–Heimer Kabir (JH) faults are shown by thickened lines. The transverse faults in the segment D are shown by bold lines (after Abou Romieh *et al.* 2009); that is, faults: B, Bweitieh; H, Harmushiyeh; K, Kasra; M, Masrab; T, Tibni; and Tr, Treif. Hachures on fault lines are directed to downthrown sides. Grey dotted lines border the segments of the valley. Grey bands demonstrate the approximate position of the composite geomorphological profiles (Fig. 3). The black triangle shows location of the geophysical profile across the Euphrates Fault.

Table 1. *Chrono-stratigraphy of the Late Cenozoic Euphrates terraces and deposits*

Terrace	Height, m	Max registered thickness of the alluvium, m	Archaeology	Inferred age
$Q_{3-4}0$, recent channel and flood plain	0–5	5	Neolithic and later	Late Pleistocene and Holocene
Q_2I	7–15	11	Early–Middle Palaeolithic (Levallois or 'Lelallois-like' material) [D*]	Middle Pleistocene, older, than *c.* 0.4 Ma
Q_1II	15–25	14	Acheulian	The late part of Early Pleistocene, older, than *c.* 0.7 Ma
Q_1III^a	30–45	5	Khattabian [D]	The earlier part of the Calabrian
Q_1III^b	45–60	18	None	Early Pleistocene, older, than *c.* 2.12 Ma [D]
N_2^2IV	80–100	>20	None	Late Pliocene, older, than *c.* 2.8 Ma

*[D] is reference to the paper of Demir *et al.* (2007).

range from tens of centimetres to 1 m for the terraces situated near the Euphrates, but could increase up to $\pm$ 2 m for localities situated several kilometres farther from the river. In these cases, we controlled the results using a combination of GPS measurements and data from the 3″ model of topography SRTM (Shuttle Radar Topography Mission) and by levelling relative to the trig points. The individual terraces were differentiated by a combination of field observations and the analysis of the SRTM data. The terraces were then correlated with our chrono-stratigraphic scheme (Table 1) based on dating using radio-isotopic and archaeological methods, coupled with information on the local sequences and the altitudes of the terraces in the part of the valley studied.

Euphrates valley between the Assad Reservoir and the town of Abou Kamal

Ponikarov *et al.* (1967) noted that the Euphrates valley consists of broad segments with a relatively simple structure and narrower segments with a more complicated structure. Three of the wide segments are located in the ESE-trending and SE-trending parts of the valley, as follows: A – near the Assad Reservoir (A′) and downstream the Al Tabqa Dam up to the Rasafeh valley (A″); C – from the Balikh River mouth to the Halabiyeh– Zalabiyeh area; and E – from Deir Az-Zor to the Abou Kamal area (sub-segments É and E′). These are separated by segments with a more complicated structure: B – between the Rasafeh and Wadi El Faid valleys and the Balikh River mouth; and D – the Halabiyeh–Zalabiyeh area.

We use the following abbreviations to describe the river valley segments: H – altitude of terrace; h – elevation above the Euphrates water level; M – total thickness of the Euphrates gravel; M′ – thickness of alluvium observed in outcrop; m – thickness of the upper fine-grained part of the alluvium; and s – site of observation.

From the Assad Reservoir to the Rasafeh valley and Wadi El Faid (Segment A)

The lower terraces are flooded in the Assad Reservoir area (Fig. 3a′). On the southwestern side of the reservoir, Eocene carbonates are covered by a large outcrop of soft conglomerates with sand lenses. This gravel forms terrace IV near the river bank. Downstream the height decreases from $H = 360$ m

Fig. 3. Principal geomorphological profiles across the segments of the Euphrates valley: (**a**′), Assad Reservoir area; (**a**″), between Ad Tabqa Dam and Rasafeh–El Faid Fault; (**b**), Ar Raqqa area; (**c**), between Nahr El Balikh and the Halabiyeh lava field; (**d**), the Halabiyeh–Zalabiyeh area; (**e**′), between Deir Ez-Zor and Mayadin; (**e**″) around Abou Hammam. The approximate position of the profiles is shown in Figure 2 by the grey band.

Geological Society, London, Special Publications published online September 6, 2012 as doi: 10.1144/SP372.4

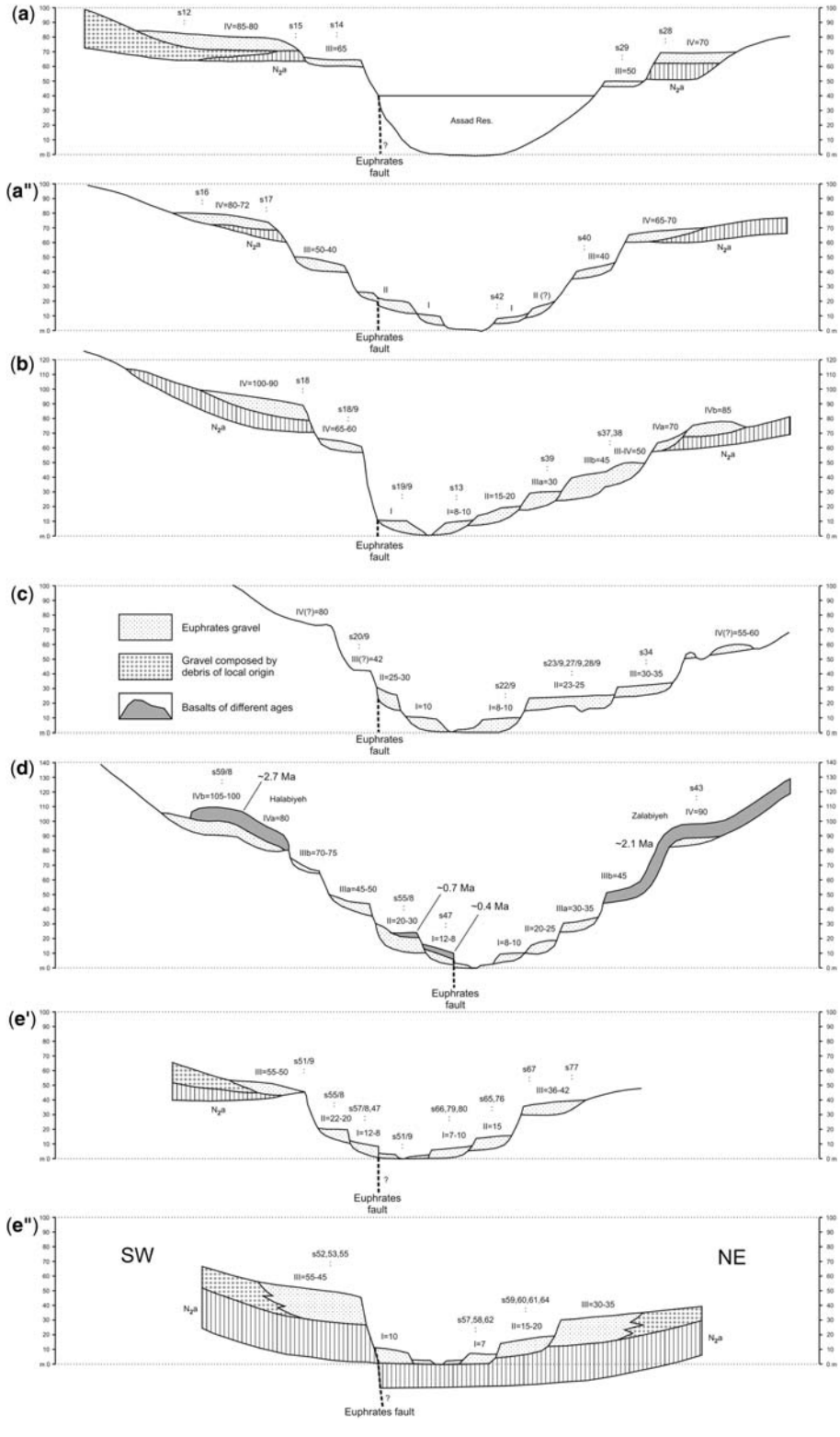

($h = 80–85$ m above the former Euphrates level) to $H = 350$ m ($h \approx 80$ m). At *c.* 10 km from the river bank, the surface begins to rise gradually up to 370–390 m. The thin ($\leq 15–20$ m) unit N_2^a disappeared in some places. This is composed of clays and silts, with interbeds of marl and limestone and lenses of pebbles in the upper part. Euphrates alluvium ($M \approx 10$ m) overlies the alluvium of non-Euphrates origin (*c.* 10–12 m), as seen in a section of terrace IV 12 km to the SE of the village of Maskaneh (s 12). The non-Euphrates gravel contains the Palmyride material that was transported locally by ephemeral streams. The non- Euphrates gravel also makes up the continuation of the terrace IV to 370–390 m. The thickness of the terrace IV alluvium reduces to the SE and then wedges out in s 15 ($H = 343$ m). Terrace III is identified further SE (s 14; $H = 332$ m; $h \approx 65$ m; $M' \approx 10$ m).

Terraces IV and III were identified in the north-eastern bank of the reservoir. There, the Euphrates pebbles ($M \approx 10$ m) overlie the unit N_2^a (*c.* 15 m), covering Palaeogene carbonates in the terrace IV section (s 28; $H = 338$ m; h $\approx$ 70 m). Terrace III (s 29; $H \approx 317$ m; $h \approx 50$ m) is composed of the Euphrates gravel overlying Palaeogene rocks.

On the southern side of the Euphrates valley, between Al Tabqa Dam and the mouths of the Rasafeh River valley and Wadi El Faid (Fig. 3a″), the cover of terrace IV is composed of soft Euphrates conglomerates with lenses of sandstones, especially in the upper part of the section. This terrace lowers in altitude from $H = 320$ m ($h \approx 80$ m) in the west (s 16) to $H = 310$ m ($h \approx 72$ m) in the east (s 17). This lowering can be partly explained by the later erosion, because the sand-rich and silt-rich upper part is absent at s 17. On the northern side of the valley, the height of terrace IV is $h = 68–70$ m. The height lowers up to *c.* 40 m to Wadi El Faid (ss 40 and 41; $M > 10$ m). Near the Wadi mouth, conglomerates cover the unit N_2^a. The terrace I ($h = 9–10$ m) consists of pebbles with sand lenses (s 42).

Around the town of Ar Raqqa between the Rasafeh and El Faid valleys and the mouth of the Balikh River (segment B)

The southern side of the valley forms a WNW-trending straight-line scarp, which separates the channel, flood plain and terrace I ($h = 6–10$ m) from higher topographic levels. South of the scarp, a flat surface is covered by pebble and rises to the south. The smoothed scarps separate the terraces III (s 18/9; $H = 300$ m; $h \approx 63$ m; $M = 7$ m) and IV (s 18; $H = 325–330$ m; $h \approx 90$ m; $M > 20$ m), covered with Euphrates pebbles, from the upper level ($H = 360–370$ m; Fig. 3b). The 360–370 m high-level pebbles probably represent the Rasafeh valley delta, composed by the Palmyride-derived clastic material.

In the northern side of the valley, the Euphrates terraces I ($h = 6–10$ m) and II ($h = 15–25$ m) occupy the 5 km-wide area in and around the town of Ar Raqqa. The Khuzayma Plateau is situated to the north of this. Its flat surface is formed by the sub-levels of the Euphrates terrace IV ($H = 302–319$ m; $h = 70–85$ m). These surfaces are covered by the 'Balikh Upper Conglomerate' (Besançon & Sanlaville 1981). Demir *et al.* (2007) proved a Euphrates origin and also reported a possible fragment of the Euphrates terrace IV ($h = 60–65$ m) on the left bank of the Balikh River. The most characteristic lower terraces are III–IV ($h \approx 55–60$ m) and III^b (ss 37 and 38; $H = 277–284$ m; $h \approx 45$ m; $M \leq 18$ m). The terrace III^a (s 39; $H = 269$ m; $h \approx 30$ m) is composed of Euphrates pebbles overlying a Tortonian-aged base in the left bank of Wadi El Faid near its mouth. Therefore, the left side of the valley in segment B is characterized by splitting of terraces IV and III into sub-levels. Splitting into sub-levels has also affected terrace II, assuming the upper sub-level there is represented by terrace III^a.

Between the Balikh River and the Halabiyeh–Zalabiyeh area (segment C)

A cross-section of the valley is asymmetrical: its central part (channel, flood plain and the terrace I) is bordered from the south by a steep straight-line scarp. The associated terraces are narrower and more fragmentary, with steeper slopes on the southern side of the valley, compared with the northern side. Fragments of the terrace II ($h \approx 25–30$ m) were identified locally along the scarp on the southern side of the valley. A gently rolling surface made up of Tortonian deposits lies above the scarp. The terrain rises from the Euphrates to 350 m ($h \approx 120$ m) in the west and 320 m ($h \approx 100$ m) in the east. Near the scarp, flat erosional terraces are nested into the plain in some places: IV? ($h \approx 80$ m), III^b? ($h \approx 70$ m) and III^a? ($h = 42–45$ m; s 20/9) (Fig. 3c).

On the northern side of the valley, the terrace I is 8–10 m high. Its cover ($M = 4.5$ m) overlies the Messinian-aged clayish sands (s 22/9). The terrace II sections (ss 22/9, 23/9 and 28/9; $h = 23–24$ m; $M \leq 10$ m) are composed of Euphrates alluvium, overlying the eroded surface of the N_2^a silts, marly clays, marls and gypsum. In ss 23/9 and 28/9, we observed sinkholes up to several metres wide and 3 m deep in the N_2^a surface, infilled with Euphrates gravel underlying the terrace II alluvium. The terrace III cover (s 34; $H = 256$ m; $h \approx 30–35$ m;

$M' = 6$ m) consists of Euphrates pebbles with silts in the upper part. The cover of terrace IV ($h = 55–60$ m) also comprises pebbles in the east of the segment C, opposite the village of Maadan Jadid (Ponikarov 1964).

The Halabiyeh–Zalabiyeh area (segment D)

The ages of the terraces in this area were determined by dating of the overlying basaltic flows and by archaeological findings within the alluvium (Besançon & Sanlaville 1981; Copeland 2004; Sanlaville 2004; Demir *et al.* 2007; Trifonov *et al.* 2011). Cross-sectional asymmetry is again characteristic of this segment, although the steep erosional scarp is only present in the southeastern part of the segment. The terrace I is usually 8–10 m high in both banks of the river, but reaches 12 m near the villages of Maadan Jadid (Besançon & Sanlaville 1981) and Ayash (Trifonov *et al.* 2011). The altitudes of the other terraces differ on opposite sides of the valley (Fig. 3d).

On the southwestern side, the terrace II ($h = 20–30$ m) was identified westwards of the village of Maadan Atiq, near the village of Tibni, westwards of the village of Treif (s 45), and westwards of the village of Ayash. The terrace II section is exposed in a quarry to the SE of the village of Ayash (s 55/8; $h = 20–23$ m; $M' = 12–14$ m; $m = 2–4$ m). The terrace III^a ($H = 265–270$ m; $h = 45–50$ m) is composed of Euphrates alluvium to the east of the village of Maadan Jadid (Copeland 2004; Demir *et al.* 2007). The terrace III^b ($h = 70–75$ m) was identified above Maadan Jadid. On the northwestern flank of the Halabiyeh lava field, a fragment of the terrace III^b has been eroded down to $h \approx 65$ m (s 59/8). Relics of the alluvium cover are <30 cm thick. Terrace IV underlies the Halabiyeh basalts. Its cover is composed of the soft Euphrates conglomerates in the northwestern side of the lava field ($H \approx 305$ m; $h \approx 100$ m; $M \approx 12$ m). The conglomerates continue to the west of the lava field at an altitude $H \approx 310$ m ($h \approx 105$ m), whereas the terrace lowers to $h = 85–80$ m further west. The base of the basalts is also at *c.* 80 m high in the southeastern part of the Halabiyeh lava field. These variations could in principle reflect, either differentiation of the terrace IV to specific sub-levels (Demir *et al.* 2007), or its deformation (Abou Romieh *et al.* 2009).

On the northeastern side of the Euphrates valley, the terrace II ($h \approx 20–25$ m) could be identified along the southern flank of the Zalabiyeh–Kasra lava field between the villages of Zalabiyeh and Kasra (Besançon & Sanlaville 1981). Terrace III^a ($H \approx 230–240$ m; $h \approx 30–35$ m; $M' = 6$ m; $m = 1$ m) is reported to the east of Kasra (Copeland 2004) and is also present east of the village of Harmushiyeh. Terrace III^b ($H \approx 250$ m; $h \approx 45$ m) underlies the Zalabiyeh basalts near the village of Zalabiyeh. A fragment of the terrace III^b? ($H \approx 245$ m; $h = 35–40$ m) was identified near the village of Jazira to the west of the lava field (Demir *et al.* 2007). The basalts cover terrace IV (s 43; $H = 290–295$ m; $h = 85–90$ m) north of the village of Zalabiyeh. The Euphrates gravel of this terrace ($M \approx 6$ m) overlies the Tortonian. Splitting of the terraces III and perhaps also of terrace IV is, therefore, characteristic of the Halabiyeh–Zalabiyeh area.

From the town of Deir Az-Zor to the area of village of Abou Hammam (segment E)

Asymmetry of the valley, with the southwestern side being steeper than the northwestern side, is illustrated by an en echelon row of scarps that are located on the southwestern side of the valley, between the village of Treif and the town of Abou Kamal. These scarps are less straight than the scarp between Ar Raqqa and Halabiyeh.

Between the village of Ayash (town of Deir Az-Zor) and the town of Mayadin (Fig. 3e′), on the southwestern side of the Euphrates valley, the terrace I section ($h = 8–12$ m; $M \leq 11$ m; $m \leq 5$ m) is exposed near the village of Ayash (Demir *et al.* 2007; Trifonov *et al.* 2011). The same terrace is *c.* 10 m high in the town of Deir Az-Zor. The terrace II is 20–23 m high in the quarry east of the village of Ayash. The upper flat surface, composed of Messinian sediments (Ponikarov 1964), is taken as an eroded part of terrace III, as seen above Deir Az-Zor (ss 51/9 and 68; $H = 235–240$ m; $h \approx 45$ m). To the SW this terrace evolves into a gentle valley slope. Southeastwards, near the village of Buqros and the town of Mayadin, the terrace III ($H \approx 240$ m; $h = 50–55$ m) is composed of sands, including small Euphrates pebbles in higher interbeds (ss 69 and 70). Euphrates pebbles and sands with basal breccias overlie the N_2^a silts, gypsum and limestone (s 71). The Euphrates pebbles with sandy loam lenses, corresponding to the terrace II (s 70; $h \approx 20$ m), are nested into terrace III (near Buqros). On the northeastern side of the Euphrates valley, terrace I ($h = 6.5–10$ m; ss 80, 79 and 66) consists of the Euphrates pebbles and sandy loam. The terrace II ($h \approx 14–15$ m; $M' \approx 6$ m; $m = 1–1.5$ m) rises above terrace I by 5–7 m. The base of terrace III ($h = 35–40$ m) is composed of Messinian sediments, while the terrace cover ($M \leq 10$ m) consists of Euphrates pebbles with lenses of sand, enriched in silt in the upper (1–2 m) part (ss 67 and 77).

Around the village of Abou Hammam (Fig. 3e″), the height of terrace I does not exceed 10–12 m in

the southwestern side of the valley. The terrace III ($H \approx 230$ m; $h = 50–55$ m) is separated by a steep scarp from the terrace I and then evolves into a gentle slope to the SW and while lowering gently to the SE (ss 53 and 52; $H \approx 220$ m; $h = 45–50$ m). The terrace III cover (>10 m) overlies the unit N_2^a and is composed of Euphrates pebbles with conglomerate–breccia in the base and interbeds of sand and silt. On the northeastern side of the valley, terrace I ($h = 6–8$ M) consists of the Euphrates pebbles, sand and silt. Terrace II (ss 59–61, 63 and 64; $h = 14–20$ m; $M \leq 10$ m) is composed of Euphrates pebbles, enriched in sand and silt in the upper part. The cover of terrace III consists of sand and pebbles. Terrace III ($H = 203–213$ m; $h \approx 30–35$ m) evolves gradually into the gentle slope of the valley to the NE.

The Late Cenozoic Euphrates Fault

The Euphrates Fault cuts the crystalline basement and the Palaeozoic units of the sedimentary cover, but was considered to be inactive thereafter (Ponikarov *et al.* 1967). However, the data presented here show that the Euphrates Fault was active during the Late Cenozoic, within the east-trending and SE-trending segments of the Euphrates valley between the Assad Reservoir in the west and Abou Kamal in the SE.

Location and vertical offsets of the young fault

The location of the young fault zone is marked by en echelon rows of steep linear or arched scarps, striking along the south-southwestern side of the Euphrates valley. The scarp between Ar Raqqa and the Halabiyeh lava field is the most distinct and straight. In the northwestern part of this segment (s 19/9), we found an offset of Tortonian-aged layers, which could be interpreted as a normal fault or a landslide (Fig. 4a). The fact that opposing sides of different segments of the Euphrates valley are made up of almost horizontally stratified deposits of different ages supports the existence of a longitudinal normal fault or flexure. Between Ar Raqqa and the Halabiyeh lava field, the southern side of the valley is composed of Tortonian deposits, whereas the northern side is composed of the unit N_2^a and, eastwards, Messinian deposits. A comparable relationship, with Upper Tortonian juxtaposed with Messinian, can be observed in the Ayash–Deir Az-Zor area. Between the Khabour River mouth and Wadi Dkhenet Suwab, the northeastern side of the valley consists completely of Euphrates alluvium above the lower terraces, but it is underlain by the unit N_2^a in the southwestern side. Petrov and Antonov (1964) demonstrated a vertical offset of Pliocene layers in a geological cross section of the Euphrates valley, near Abou Hammam.

We have correlated the heights of the terraces on the opposite sides of the Euphrates, separately for each river segment. This shows that the synchronous terraces are systematically lower on the left (northeastern) side of the river relative to the right side (Table 2; Fig. 3). The difference in height does not exceed 10 m on the opposing sides of the Assad Reservoir (Fig. 3a′), but reaches 20–25 m (30 m?) in the more southeastern cross-sections. We interpret this height difference as the offset along the Euphrates Fault. The offset is not observed below

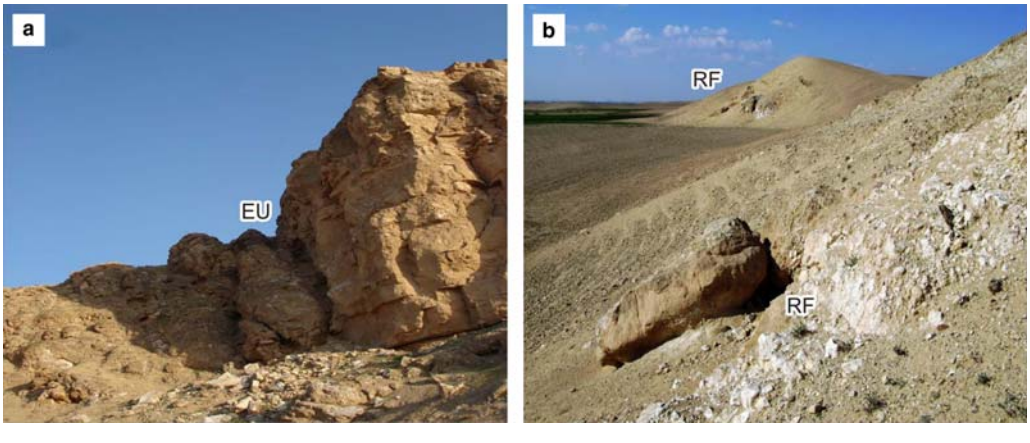

Fig. 4. Neotectonic features of the Euphrates valley: (**a**) the Euphrates Fault (EU) as a scarp cutting the Tortonian on the rear side of the terrace I opposite the town of Ar Raqqa (s 19/9); (**b**) the Rasafeh–El Faid fault zone (RF) cutting the Tortonian on the southern side of the Euphrates valley (s 18/9). Photographs by V. G. Trifonov.

Table 2. *Correlation of height of the terraces in the right and left Euphrates banks and approximate estimate of the rate of vertical motion on the Euphrates Fault*

Segment of the Euphrates Valley	Terrace	h, right side, m	h, left side, m	Difference of height, m	Rate of motion on fault, m/Ma
A'. The Assad Reservoir, eastern part	N_2^2IV	80–85	70–75	~ 10	~ 4**
A". Between Al Tabqa Dam and mouths of the Rasafeh Valley and Wadi El Faid	N_2^2IV	~ 80 in the W	98–70 in the W	~ 10	~ 4
		~ 70 in the E	~ 40 in the E	~ 30	~ 11
B. Between the Rasafeh Valley–Wadi El Faid and the Balikh River	N_2^2IV	~ 90	70–85	5–20	~ 7
	Q_1III	~ 63	III^b = 45	18	~ 8
C. Between the Balikh River and the Halabiyeh–Zalabiyeh area	Q_1III^b?	70–75	50–60	15–20	~ 8
	Q_1III^a?	42–45	30–32	12–13	~ 8
	Q_1II	25–30	23–24	2–6	~ 5
D. Halabiyeh–Zalabiyeh area, including villages of Maadan, Kasra and Ayash	N_2^2IV	100–105	85–90	15–20	~ 7
	Q_1III^b?	70–75	45–50[D]*	~ 25	~ 11
	Q_1III^a?	45–50 [D]	30–40 [D]	~ 15	~ 9
	Q_1II	20–30	20–25	0–5	~ 4
E'. From Deir Az-Zor to Mayadin	Q_1III	50–55	35–40	~ 15	~ 7
	Q_1II	~ 20	14–15	5–6	~ 8
	Q_2I	~ 10	6.5–10	0–3.5	~ 8
E". Around the village of Abou Hammam between the Khabour River and Wadi Dkhenet Suwab	Q_1III	45–55	30–35	15–20	~ 8
	Q_1II	–	14–20	–	
	Q_2I	10–12	6–8	~ 4	~ 10

*[D] is reference to the paper (Demir *et al.* 2007).
**Principles of estimation of the rate of motion on the Euphrates Fault are described in the text.

the mouth of Wadi Dkhenet Suwab and is certainly absent near the town of Abou Kamal (Figs 1 & 2). The offset of the terraces indicates the amount of movement on the fault since the end of the Late Pliocene (time of the terrace IV formation). Terraces IV and III are offset a greater distance (up to 20–25 m and possibly 30 m) than terrace II (3–6 m) (Figs 5 & 6). This implies that multiple vertical movements have taken place on the fault. We did not identify any offset of terrace I in segments A–D. However, the small (to 2–4 m), but systematic lowering from the right side of the valley to the left side in segment E suggests that the Euphrates Fault was still active after mid-Pleistocene time.

Geophysical profile across the Euphrates Fault

The geophysical profiling was carried out along a 300 m-long line 3 km south of Ar Raqqa (Fig. 2). The coordinates of the profile are from N 35.89718° and E 39.00735° to N 35.89484° and E 39.00581°. The profile intersects the steep scarp on the southern side of the Euphrates valley along a small incised ravine. Three methods were used: (1) dipole axial sounding; (2) seismic correlation refraction method (CRM); and (3) georadar.

The dipole axial sounding was carried out using geoelectrical equipment of the ERA-MAX, produced in the NPO ERA (St Petersburg, Russia). The equipment operates with stable electrical power with a frequency 625 Hz. The electrical sources were located 10 m apart between the generator geoelectrodes A and B in the land surface. The distance between the gouge dipole geoelectrodes M, N, etc., was also 10 m. The maximum length of the system used was 150 m. The current in the wire varied from 20 to 200 ma, depending on the geoelectrical properties of the ground layers in depths up to *c.* 1/4 of the line length (≤40 m). The field-data that were obtained were processed using the mini-computer HP iPAQ. To aid visualization of the data, the method of designing apparent

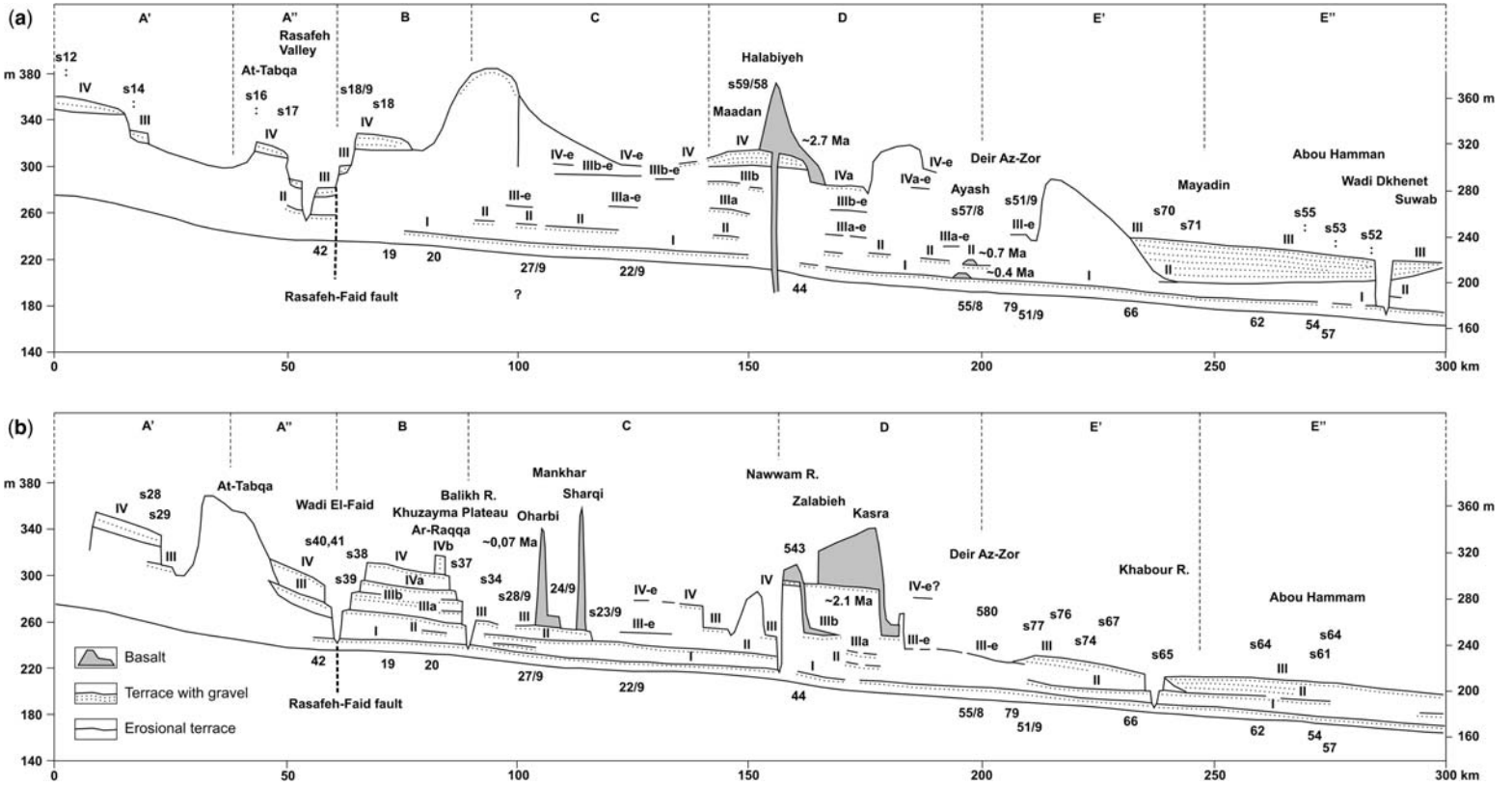

Fig. 5. Longitudinal geomorphological profiles along the southwestern (**a**) and the northeastern (**b**) sides of the Euphrates valley.

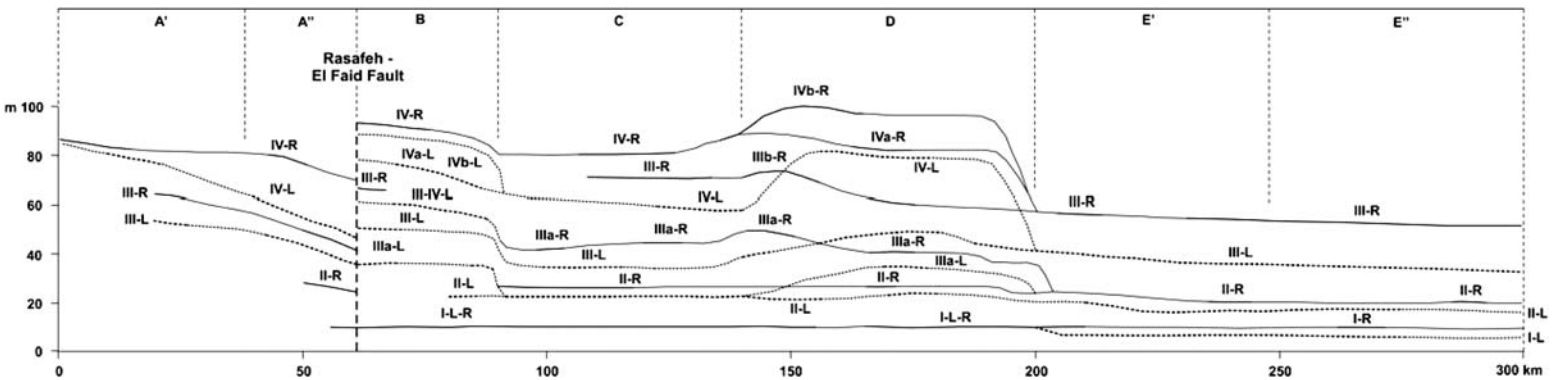

Fig. 6. Geomorphological profile along the Euphrates valley, based on combined evidence; 'r' is the right bank and 'l' is the left bank of the valley.

resistance cross-sections was used. Designing the cross-section allows an estimation of the geoelectric situation for the profile as a whole. The apparent resistance was calculated according to the formula:

$$\rho_k = k\frac{\Delta U}{I} \quad (1)$$

where

$$k = \frac{2\pi}{(1/|\mathrm{BM}| - 1/|\mathrm{AM}| - 1/|\mathrm{BN}| + 1/|\mathrm{AN}|)}$$

The CRM was used for an analysis of seismic data involving the initiation of seismic waves by hammer shocks. To register the seismic signals, 24 channel digital seismic station 'Seismolog 24' (made in Khabarovsk, Russia) was used with vertical geophones and a 20 Hz frequency body. The distance between the geophones was 5 m and the whole length of the seismic line with geophones, 115 m. Four sites for hammer shocks were used. The signals were registered by geophones, situated at distances of 2.5–30 m from the site. The recording time was 1024 ms with 0.5 ms discretion of records.

To reduce the potential for errors, the measurements were repeated several times at the same site. The seismograms obtained were summed to reduce the noise pollution and increase the signal strength. Further interpretation was made using standard techniques of processing of the CRM. As a result, a seismic velocity cross-section was obtained for the profile as a whole.

The georadar investigations were carried out using the equipment OKO-II, produced by the NPO 'Logis' in Ramenskoe, Russia. The nonprotected antenna block 'Triton' with dipole antenna frequency 50 and 100 MHz was used allowing a 20 m depth of penetration. The signals were registered using an 'Asus' note book. The profile was studied twice: with the 100 MHz antenna frequency during the forward direction and with the 50 MHz during the reverse direction. An estimate of the field radargrams was made by the dedicated program, GeoScan NPO 'Logis'. The data obtained by the three methods were exported to the AutoCAD format for further combined interpretation.

The geophysical profiling as a whole confirmed the existance of a fault zone made up of four almost vertical main strands that offset a surface of Tortonian deposits, together with two smaller ruptures within the Tortonian unit. The southern strand (1 in Fig. 7d) coincides with the topographic scarp on the southern side of the valley near the profile and offsets the surface of Tortonian deposits to *c.* 15 m (the southern side is uplifted). To the north, the next strand shows a small rise in the surface of Tortonian deposits on the southern side. This strand penetrates the Quaternary deposits as shown by a small, gentle scarp in the terrace I surface (2 in Fig. 7d). The fault strand 2 was clearly active after terrace I formed. The third and fourth strands border a narrow horst, which is not seen in the land surface (3 and 4 in Fig. 7d).

In summary, the geophysical studies show that a young fault has influenced the scarp bordering the Euphrates channel, the flood plain and terrace I in the south. The Tortonian surface is uplifted on the southern side of the fault zone as a whole up to *c.* 25 m relative to its northern side. The actual offset is $\geq$30 m, because the southern end of the profile is now *c.* 5 m lower than the eroded Tortonian surface on the southern side of the scarp near the profile studied.

Transverse faults and zones of deformation in the Euphrates valley region

The Euphrates valley forms a *c.* 7 km northward bend near the mouths of the Rasafeh and El Faid tributaries. The almost vertical fault with its uplifted eastern side, eroded into Tortonian sediments, can be traced along the eastern slope of the Rasafeh valley (Fig. 4b). Terrace IV becomes lower in segment A″ on the southern side of the Euphrates valley eastwards from $h \approx 80$ m (trigpoint 351 m and s 16) to $h = 72$ m (s 17). East of the Rasafeh valley, the terrace rises sharply to $h \approx 90$ m (Fig. 5a). Similar changes were also observed along the northern Euphrates bank. Terrace IV becomes lower in segment A″, eastwards from $h = 70–75$ m (s 28a) to $h = 68–70$ m (trig point 305 m near the village of Ash-Shara) and, perhaps, $h \approx 40$ m (s 41), but reaches $h = 70–85$ m to the east of the El Faid Wadi, on the Khuzayma Plateau (Fig. 5b). Obviously, the fault zone with the uplifted eastern side strikes along the Rasafeh valley and the El Faid Wadi (Fig. 6). The uplifted side is characterized by splitting of terraces III and IV. An en echelon continuation of the fault zone is observed on the eastern side of the Balikh River valley (RF2 in Fig. 1). Its more northern continuation is shown as a north-trending normal fault in the active fault map of Turkey (Şaroğlu *et al.* 1992) (RF3 in Fig. 1). To the SW, the Rasafeh–El Faid zone follows the Rasafeh valley, where possible strands of the fault zone border a narrow and shallow topographic depression. Further SW (RF4 in Fig. 1), the inferred fault zone continues via the Butma–Kastal fault zone, with a small Quaternary uplift of the southeastern side and a probable sinistral component of motion. The Butma–Kastal–Rasafeh–El Faid fault system separates the Aleppo Block from the Palmyrides and the Mesopotamian Foredeep. This fault system is

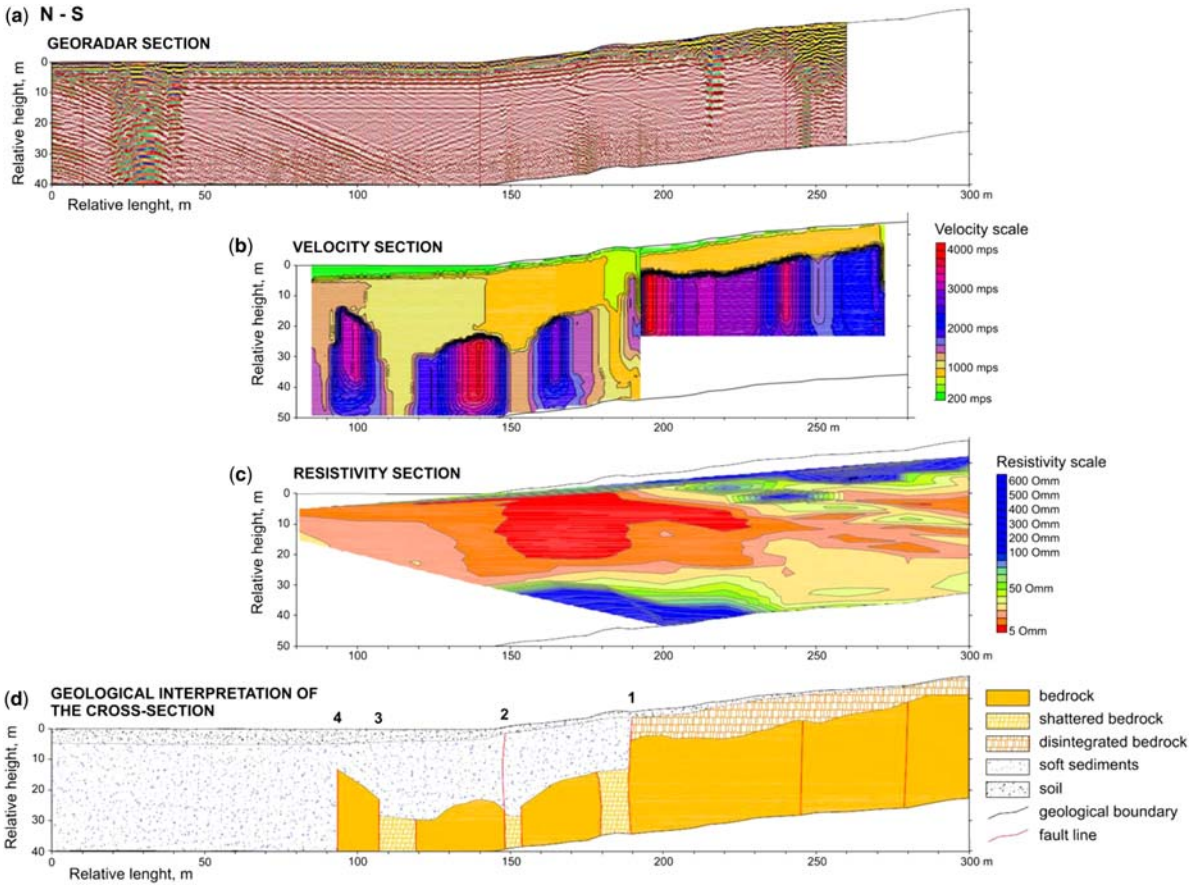

Fig. 7. Results of the geophysical profiling across the Euphrates fault zone in the southern bank of the Euphrates River, 3 km south of the town of Ar Raqqa: (**a**), Georadar section; (**b**), section of velocities of the refraction waves (the correlation refraction method); (**c**) geoelectric resistance section (the dipole axial sounding); and (**d**) geological interpretation. The visible vertical offset of the Tortonian surface is *c.* 15 m on the fault strand 1. The offset on strand 2 is smaller. Strand 2 ruptures the terrace I gravel and is reflected by small gentle scarp in the land surface. Strands 3 and 4 border narrow horst which is not reflected in the land surface. The total offset of the surface of the Tortonian on all strands of the Euphrates fault zone is not less than *c.* 25 m.

Geological Society, London, Special Publications published online September 6, 2012 as doi: 10.1144/SP372.4
LATE CENOZOIC TECTONICS OF THE EUPHRATES

located on a continuation of the Serghaya left-lateral active fault (SH in Fig. 1), branching out the DST.

The eastern margin of the Aleppo Block is cut by several other young NNE-trending faults. One of these was traced from the Beer Jaber area to the village of Heimer Kabir. This is a normal fault with a small half-graben on the western side, infilled with Pliocene pebbles and other stones composed of local rock debris (ss 30–33). Normal faults of the same trend are inferred within the Euphrates valley, southwards to the village of Shireen (Ponikarov 1964).

Another type of transverse deformation of the Euphrates valley is seen in the Halabiyeh–Zalabiyeh area (segment D), which is situated in the north-eastern pericline of the Palmyride Bishri anticline. Late Cenozoic activity of this segment is implied by the presence of basaltic volcanism, uplift and splitting of terraces III and IV (Figs 5 & 6 and Table 2). Abou Romieh *et al.* (2009) reported the Masrab–Kasra, Tarif (Treif), Bweitieh–Harmushiyeh and the Tibni transverse faults based on vertical offsets and deformation of terraces and lava flows in the Halabiyeh–Zalabiyeh area. The offsets are most evident in the right (southwestern) side of the valley, where their existence was confirmed, with the same slip polarity, by seismic profiling (Litak *et al.* 1997); also, some faults are actually exposed. The Masrab Fault exhibits a reverse offset that disappears to the NE. Some previous estimates of fault offsets are incorrect, because terraces of different age were correlated. For example, the observed 30–50 m height contrast on both sides of the Masrab Fault does not reflect the offset of single terrace.

The Masrab–Kasra Fault, with its uplifted northwestern side, deforms part of the Zalabiyeh–Kasra basaltic field. However, 10 km further NE, plateau basalt NW of the fault line is at the same level as gypsum bedrock to the SE (Abou Romieh *et al.* 2009). The Bweitieh–Harmushiyeh Fault disappears within the southern part of the Zalabiyeh–Kasra lava field, while the Tibni Fault disappears on the Halabiyeh plateau.

Offset and deformation of the Euphrates terraces fix the movements on the Rasafeh–El Faid fault zone and the Halabiyeh–Zalabiyeh pericline of the Bishri anticline as being from the time of formation of terrace IV (N_2^2) until the period of formation of terrace II (late Q_1). The Halabiyeh–Zalabiyeh pericline is possibly structurally similar to the transverse folded–faulted zone, which terminates the Euphrates Fault at its intersection with the Euphrates valley near Abou-Kamal (Ponikarov 1964; Ponikarov *et al.* 1967).

The presence of transverse ruptures is indicated by liquefaction structures and local deformation of the Euphrates terraces. Dykes and micro-diapirs are filled with sand and pebbles. There are also small folds, thrusts and reverse faults with offsets up to several tens of centimetres (Fig. 8). Some of these features deform only the lower parts of the terrace section, that is, they formed during the alluvial accumulation. These ruptures only occur within the transverse zones of faulting and deformation: that is, the terrace III^b on the eastern side of the Rasafeh–El Faid fault zone (s 38) and the terrace II seen near the village of Treif to the SE of the Halabiyeh lavas (s 45), at the quarry to the SE of Ayash (s 55/8) and at Abou-Kamal (s 49).

Discussion: Late Cenozoic evolution of the Euphrates valley

During the Early Miocene, a shallow-marine strait linked the proto-Mediterranean and Mesopotamian marine basins in northwestern Syria and the adjacent part of Turkey (Ponikarov *et al.* 1967). Alluvial conglomerates with pebbles of igneous and metamorphic rocks from the inner zones of Turkey also occur in the Kahramanmaraş area, where they have been dated as end-Early Miocene (Derman 1999). A river delta may already have transported debris into the sea in this area (Demir *et al.* 2007). Complex relationships between marine deposits, alluvium and sub-aerial basalts demonstrate tectonic instability corresponding to a phase of deformation, as documented in northwestern Syria (Rukieh *et al.* 2005). A linkage between the Mediterranean and Mesopotamian marine basins was restored during the Helvetian, but was terminated at the beginning of Late Miocene because of folding in the Palmyrides and a relative rise of the Aleppo Block, coupled with renewed sub-aerial basaltic eruption (Ponikarov *et al.* 1967; Trifonov *et al.* 2011). The lagoon and coastal marine sediments, together with evaporites, accumulated in the Syrian part of the Mesopotamian basin during the Tortonian. Lacustrine deposition followed during the Messinian, which allowed aprons of fine-grained sediments to accumulate along the basin margins, derived from the still weakly uplifted anticlines of the Palmyrides, Abdel Aziz and the Marginal Folds of Turkey (Ponikarov *et al.* 1967). The axial part of the Mesopotamian Foredeep, in which the greatest thickness of the Miocene deposits accumulated, partly coincided with the area of the future Euphrates valley (Fig. 1; Rukieh *et al.* 2005). During the Pliocene the area of maximum subsidence moved northward, to the area to the east of the town of Al Qamishli, where the Pliocene reached 1000 m in thickness. Residual depressions with sparse sedimentation of the former type (unit N_2^a) remained in the Euphrates area. Surrounding weakly uplifted plains were blanketed by clastic material derived from the adjacent folded zones. This material became coarser as the folds and deformed zones rose and became more accentuated.

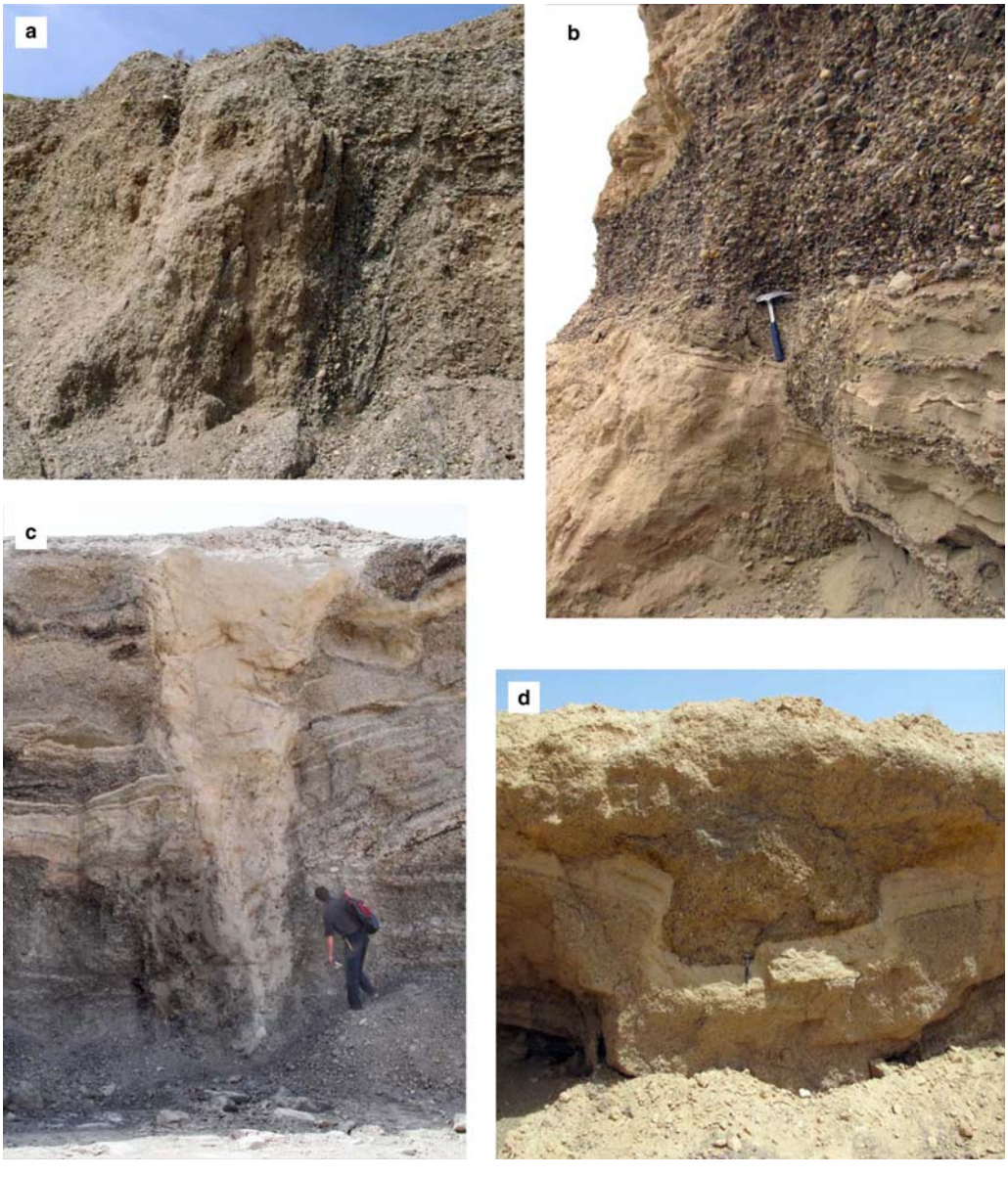

Fig. 8. Sand and gravel dykes and secondary tectonic deformation affected terrace alluvium. (**a**) Gravel dyke cutting terrace III^b on the eastern side of the Rasafeh–El Faid fault zone, left bank of Euphrates (s 38); (**b**) reverse micro-fault cutting terrace II on the northeastern pericline of the Bishri anticline, the right bank of Euphrates near the village of Treif (s 45); (**c**) sand dyke cutting terrace II in the eastern part of the northeastern pericline of the Bishri anticline, the right bank of Euphrates in a quarry SE of Ayash (s 55/8); and (**d**) small fold in terrace II on the western side of the NE-trending fault zone, right bank of Euphrates in the town of Abou Kamal (s 49). Photographs by V. G. Trifonov.

In Syria, the oldest Euphrates alluvium occurs in the wide Jrablus segment of the Euphrates valley near the Syrian–Turkish border. A gently dipping river terrace-like plain occurs at $h = 80–90$ to 120 m. The section, *c.* 100 m thick, consists of clays, clayish marls, limestones, sandstones and conglomerates. Conglomerates make up a discrete layer in the base of the unit and also forms lenses in the upper part of the deposit. The unit was mapped as the N_2^a, overlying the Eocene- and Helvetian-aged

lithologies with an unconformity. The overlying basalts were inferred to be Late Pliocene (Ponikarov 1964). These deposits (N_2^a) probably correspond to the Ít Dağı gravel of the highest terrace in the Birecik segment of the Euphrates valley, just north of the Syrian–Turkish border ($h \approx 130$ m; the age is estimated as 3–5 Ma; Demir *et al.* 2008).

Downstream, between the town of Jrablus and the village of Qarah Qozaq, at least three terraces *c.* 8–70 m high are reported from the northeastern side of the valley (Sanlaville 2004). These are nested into the terrace-like plain and probably correspond to our terraces I–III. Demir *et al.* (2008) correlated the 40–45 m gravel with MIS14 or MIS16 (*c.* 500–600 ka). Demir *et al.* (2007) reported fluvial gravel ($h \approx 70$ m), covered (near Shireen) with basalts with an $^{40}Ar/^{39}Ar$ age of 8809.2 ± 72.6 ka. However, this gravel cannot be Euphrates alluvium, because it consists of clastic material of only local origin.

The fine-grained sediments with interbeds of limestone and gypsum accumulated during the epoch N_2^a, within the more southern segments of the Euphrates valley (Assad Reservoir area and further SE). Euphrates pebbles are found only in the upper part of the N_2^a sections. Therefore, the Euphrates could only have reached these local flat depressions during the end of the epoch N_2^a. The propagation was probably caused by the rebuilding of the northern part of the Dead Sea Transform, which occurred from 4 to 3.5 Ma (Rukieh *et al.* 2005, Westaway *et al.* 2006) and this, in turn, activated the faults on the eastern flank of the Aleppo Block. The new river segments were incised along renewed faults (Table 3). The propagation is documented by thin lenses of the Euphrates pebbles in the upper part of the N_2^a sections and by thick sections of the Euphrates gravels composing the terrace N_2^2IV. Large areas are covered with Euphrates gravels in the Assad Reservoir–Ar Raqqa region, reflecting the meandering of channels over a 30 km-wide flat depression, bounded by gentle slopes. Locally derived clastic material covered the Assad Reservoir to the south and probably also the right bank of the Rasafeh valley.

Movements on the Rasafeh–El Faid fault zone are documented from the time of formation of terrace IV. These movements caused the knee-shaped bend in the Euphrates valley and the splitting of terraces IV and III in the Ar Raqqa area.

Table 3. *Correlation between tectonic events, volcanism and epochs of intense incision and alluvial accumulation in the Syrian part of the Euphrates valley*

Age		Ma	Folding, faulting, uplift and intensive incision	Alluvium cycle (coarse → fine)		Volcanism
Messinian		5.0	Southern Turkey, Palmyrides			
Pliocene	Early	*c.* 4.0		N_2^a alluvium, mainly		
		c. 3.9		in Jrablus Depression		
		c. 3.6	DST, East of Aleppo Block,			
		c. 3.5	incision in east Aleppo Block	IV terrace alluvium,		
	Late	2.8		mainly in segments		
		2.6		A–D		Halabiyeh
		c. 2.5	Incision in segments A–D			
Quaternary	Early	*c.* 2.4	and upstream, IV terrace formation	III terrace alluvium, including segment E	III[b]	
		2.2				
		2.1				Zalabiyeh
		c. 1.8	Incision in segments B and D			
		c. 1.5			III[a]	
		c. 1.2	Incision in Abou Kamal			
		c. 0.9	and upstream, III terrace formation	II terrace alluvium, including Iraq		
		0.8				
	Middle	0.7				Ayash
		c. 0.6	Incision in all segments,			
		c. 0.5	II terrace formation	I terrace alluvium		
		0.4				Ayash
		c. 0.4	Incision in all segments,			
		c. 0.3	I terrace formation	Flood plain and		
	Late	*c.* 0.13		recent channel		
		c. 0.05		alluvium		Mankhar
		0				

The movements on the Euphrates Fault and the relative uplift of the land resulted in incision of the river and the transformation of the former flat bottom to the terrace IV, extending from the Assad Reservoir to the Halabiyeh–Zalabiyeh area during end-Late Pliocene–Early Gelasian time. During the accumulation of the terrace IV gravels, the Euphrates valley remained as a wide flat depression, from Deir Az-Zor downstream almost to Abou Kamal. Within this lower depression, distal facies of the Euphrates alluvium corresponding to terrace IV, formed small lenses in the upper part of the unit N_2^a. This indicates that the upper part of the unit N_2^a is younger here than in the upstream segments of the valley, and also demonstrates aggradation of the Euphrates alluvium. The coarser terrace III Euphrates gravels aggraded in the lower depression after uplift of the upstream part of the valley and the formation of the terrace IV there. Incision occurred within the lower depression after accumulation of the terrace III alluvium and transformed this into terrace III during the Early Calabrian. We have no data to indicate whether or not the Euphrates River continued during this time through the Abou Kamal transverse zone to Iraq. However, this continuation certainly existed by the end of the Early Pleistocene, because the terrace II is present in the Abou Kamal area.

Uplift and intense incision are, therefore, considered to have propagated downstream in the Syrian part of the Euphrates valley (Table 3), although we have no data to estimate the relative roles of climatic and tectonic processes. The incision began in the eastern Aleppo Block during the late Early Pliocene (*c.* 3.5 Ma). The Euphrates alluvium began to aggrade in flat depressions along the downstream segments of the future valley. The alluvium was coarse in the segments A–D, but mostly fine-grained in the segment E. Probable activity of the Halabiyeh–Zalabiyeh pericline (segment D) prevented transport of coarse debris downstream. The second pulse of incision affected segment D and upstream areas during the Late Pliocene (*c.* 2.6 Ma), while aggradation of alluvium (coarser than before) continued within segment E. Probable activity of the Abou Kamal transverse folded-faulted zone limited the supply of coarse debris downstream. The third, fourth and fifth pulses of incision affected all of the Syrian segments of the valley during the Early Pleistocene (*c.* 1.2 Ma) and the Middle Pleistocene (*c.* 0.7–0.6 and *c.* 0.4–0.3 Ma).

Segments of the Euphrates Fault formed permanent boundaries of the valley only between Ar Raqqa and Halabiyeh–Zalabiyeh area and between Deir Az-Zor and Mayadin. Elsewhere, alluvium extended onto the uplifted side of the fault. This implies that only limited segments of the fault were active during the accumulation of the alluvium. However, the fault as a whole became active during the uplift and incision of the river, leading to the formation of the terraces.

We calculated the approximate average rates of vertical movements on the different fault segments using our data on the heights of the terraces and estimates of the ages of their gravels: that is, 2.8, 2.2, 0.8 and 0.4 Ma for the terraces IV–I, respectively (see Table 2). The offsets of terraces IV and III yielded approximately the same rates, 9 ± 2 m/Ma, everywhere from the Rasafeh–El Faid fault zone to the segment E″. In segment A′ and in the western part of segment A″, the rate decreased to *c.* 4 m/Ma. This shows that the fault activity decreases westward from the Rasafeh–El Faid zone; that is, within the Aleppo Block. Offsets of terrace II indicated rates of 4–5 m/Ma in segments C and D. No offsets or deformation of the terrace I could be determined in these segments. This indicates that the fault activity decreased in the west during the Quaternary. However, faulting of the terrace I gravel on the fault strand 2 is indicated by the geophysical profiling in the segment B (Fig. 7). In the segment E, offsets and deformation of terraces II and I yielded the same rates (i.e. 9 ± 1 m/Ma) as the offsets of the terrace III. Probably the fault is still active there. These indications of young activity of the Euphrates Fault as well as activity of some segments of the Rasafeh–El Faid zone in the Rasafeh valley are confirmed by the records of historical earthquakes: 160 AD with $M_s = 6.0$ (N 34.7° and E 40.7°), 800–802 with $M_s = 6.1$ (N 35.7° and E 38.7°), and 1149 with $M_s = 6.6$ (N 35.9° and E 39.0°; Kondorskaya & Shebalin 1982; Kondorskaya & Ulomov 1999; Sbeinati *et al.* 2005).

Conclusions

Intense fluvial incision propagated downstream along the Euphrates valley during the Pliocene and Early Pleistocene, from the Syrian–Turkish border area to the Iraq–Syrian border area. During the Early Pliocene, the Euphrates River reached a small sedimentary basin near the Syrian–Turkish border. Aggradation of Euphrates alluvium began there. Because of formation (or reactivation) of faults on the eastern margin of the Aleppo Block 3.5–4 Ma, the river incised the faults during *c.* 3.0–3.5 Ma and penetrated the flat residual depression of the Mesopotamian Foredeep (between the Assad Reservoir area and the Halabiyeh basaltic field) and at times reaching a more southeasterly flat depression (almost as far as the town of Abou Kamal). The direction and incision of the valley were controlled by the Euphrates Fault, which became active. The uplift began in the western segments of the valley (between the Assad Reservoir and

Halabiyeh–Zalabiyeh areas) between the end of the Pliocene and the beginning of the Pleistocene. The uplift was reflected in incision into the former flat bottom of the valley and the formation of alluvial terrace IV. Aggradation in a flat depression continued downstream. Uplift and intense incision in this area began during the late Early Pleistocene as indicated by formation of alluvial terrace III.

Transverse zones of faulting and deformation also controlled the valley evolution. The Rasafeh–El Faid fault zone with its uplifted eastern side caused the knee-shaped bend of the Euphrates valley to the north. The Halabiyeh–Zalabiyeh pericline belonging to the Bishri anticline of the Palmyrides provided an eastern limit to the area of uplift during the Late Pliocene to the beginning of the Early Pleistocene. The southeastern boundary of the flat, wide segment of the valley was bounded by the Abou Kamal transverse zone during Late Pliocene–Early Pleistocene time. This structural feature constrained the propagation of the Euphrates River and prevented supply of coarse alluvium to the southeasterly part of the Mesopotamian Foredeep until the late Calabrian time.

V. G. Trifonov, D. M. Bachmanov, O. Ali, A. E. Dodonov, T. P. Ivanova and A. M. Al-Kafri carried out the geological and geomorphological studies and interpretation. A. A. Syas'ko, A. V. Kachaev, N. N. Grib and V. S. Imaev realized the geophysical profiling. The studies were supported by the Program 6 'Geodynamics and physical processes in the lithosphere and upper mantle' of the Department of Geosciences of the Russian Academy of Sciences, grant 11-05-00628-a of the Russian Foundation for Basic Research, and the Project 'Geodynamics of Syria' of the General Organization of Remote Sensing, Syria. The authors cordially thank Professor Alastair H. F. Robertson and two anonymous reviewers for useful comments on and corrections to the paper.

References

Abou Romieh, M., Westaway, R. *et al.* 2009. Active crustal shortening in SE Syria revealed by deformed terraces of the River Euphrates. *Terra Nova*, **21**, 427–437; http://dx.doi.org/10.1111/j.1365–3121.2009.00896.x

Barazangi, M., Seber, D., Chaimov, T., Best, J., Litak, R. D. & Sawaf, T. 1993. Tectonic evolution of the northern Arabian plate in western Syria. *In*: Boschi, E., Mantovani, E. & Morelli, A. (eds) *Recent Evolution and Seismicity of the Mediterranean Region*. Kluwer Academic, Dordrecht, 117–140.

Besançon, J. & Sanlaville, P. 1981. Apercu geomorphologique sur la vallee de l'Euphrate Syrien. *Paleorient*, **7**, 5–18.

Copeland, L. 2004. The paleolithic of the Euphrates Valley in Syria. *British Archaeological Reports, International Series*, **1263**, 19–114.

Demir, T., Westaway, R., Bridgland, D., Pringle, M., Yurtmen, S., Beck, A. & Rowbotham, G. 2007. Ar–Ar dating of Late Cenozoic basaltic volcanism in northern Syria: Implications for the history of incision by the River Euphrates and uplift of the northern Arabian Platform. *Tectonics*, **26**, TC 3012, http://dx.doi.org/10.1029/2006TC001959.

Demir, T., Seyrek, A., Westaway, R., Bridgland, D. & Beck, A. 2008. Late Cenozoic surface uplift revealed by incision by the River Euphrates at Birecik, southeast Turkey. *Quaternary International*, **186**, 132–163.

Derman, A. 1999. Braided river deposits related to progressive Miocene surface uplift in Kahraman Maraş area, SE Turkey. *Geological Journal*, **34**, 159–174.

Elias, S. A. (ed.) 2007. *Encyclopedia of Quaternary Science*. Elsevier, Amsterdam.

Golonka, J. 2004. Plate tectonic evolution of the southern margin of Eurasia in the Mesozoic and Cenozoic. *Tectonophysics*, **381**, 235–273.

Ilhan, E. 1974. Eastern Turkey. *In*: Spencer, A. M. (ed.) *Mesozoic–Cenozoic Orogenic Belts*, **1**. Scottish Academic Press, Edinburgh.

Kondorskaya, N. V. & Shebalin, N. V. (eds) 1982. *New Catalog of Strong Earthquakes in the USSR from Ancient Times Through 1977*. World Data Center A for Solid Earth Geophysics, NOAA, Boulder, CO.

Kondorskaya, N. V. & Ulomov, V. I. (eds) 1999. *Special Catalogue of Earthquakes of the Northern Eurasia (SECNE)*. Global Seismic Hazard Assessment Program, Boulder, CO. World Wide Web Address: http://www.seismo.ethz.ch/gshap/neurasia/nordasiacat.txt

Litak, R. K., Barazangi, M., Beauchamp, W., Seber, D., Brew, G., Sawaf, T. & Al-Youssef, W. 1997. Mesozoic–Cenozoic evolution of the intraplate Euphrates fault system, Syria; implication for regional tectonics. *Journal of Geological Society, London*, **154**, 653–666.

Muhesen, S. 1985. *L'Acheuleen Recent Evolue de Syrie*. British Archaeological Reports, International Series, **248**, 1–189.

Petrov, V. I. & Antonov, B. S. 1964. *The Geological map of Syria. Scale 1:200,000. Sheets I-37-XVII, XVIII*. Explanatory Notes. Ministry of Industry, Damascus.

Ponikarov, V. (ed.) 1964. Geological Map of Syria. Scales 1:200 000. Technoexport/Ministry of Industry of the S.A.R., Damascus/Moscow.

Ponikarov, V. P., Kazmin, V. G. *et al.* 1967. *Geological Map of Syria, scale 1:500,000. Explanatory Notes, Part I*. Ministry of Industry, Damascus.

Robertson, A. H. F. 2000. Mesozoic–Tertiary tectonic-sedimentary evolution of south Tethyan oceanic basin and its margins in southern Turkey. *In*: *Tectonics and Magmatism in Turkey and the Surrounding Area*. Geological Society, London, Special Publications, **173**, 97–138.

Robertson, A., Unlügenç, Ü. C., Inan, N. & Tasli, K. 2004. The Misis–Andirin Complex: a Mid-Tertuary melange related to late-stage subduction of the Southern Neotethys in S. Turkey. *Journal of Asian Earth Sciences*, **22**, 413–453.

Rukieh, M., Trifonov, V. G. *et al.* 2005. Neotectonic Map of Syria and some aspects of Late Cenozoic evolution of the north-western boundary zone of the Arabian plate. *Journal of Geodynamics*, **40**, 235–256.

SANLAVILLE, P. 2004. Les terraces Pléistocènes de la vallée de l'Euphrate en Syrie et dans l'extrême sud de la Turquie. *Archaeological Reports, International Series* **1263**, 115–133.

ŞAROĞLU, F., EMRE, Ö. & KUŞÇU, Ĭ. 1992. *Active fault map of Turkey. 1:1 000 000. Directory of Mineral Resources and Exploration*, Ankara.

SBEINATI, M. R., DARAWCHEH, R. & MOUTY, M. 2005. The historical earthquakes of Syria: an analysis of large and moderate earthquakes from 1365 B.C. to 1900 A.D. *Annals of Geophysics*, **48**, 347–435.

SHARKOV, E. V., CHERNYSHEV, I. V. *ET AL.* 1998. New data on the geochronology of Upper Cenozoic plateau basalts from northeastern periphery of the Red Sea rift area (Northern Syria). *Doklady of Russian Academy of Sciences, Earth Section*, **358**, 19–22.

TRIFONOV, V. G., TRUBIKHIN, V. M., ADJAMIAN, J., JALLAD, Z., EL HAIR, Yu. & AYED, H. 1991. Levant fault zone in the north-western Syria. *Geotectonics*, **25**, 145–154.

TRIFONOV, V. G., DODONOV, A. E. *ET AL.* 2011. New data on the Late Cenozoic basaltic volcanism in Syria, applied to its origin. *Journal of Volcanology and Geothermal Research*, **199**, 177–192.

VAN LIERE, W. J. 1960–1961. Observation on the quaternary of Syria. *Berichten van de Rijksdienst voor het Oudheidkundig Bodemonderzoek*, **10/11**, 7–69.

WESTAWAY, R. 2004. Kinematic consistency between the Dead Sea Fault Zone and the Neogene and Quaternary left-lateral faulting in SE Turkey. *Tectonophysics*, **391**, 203–237.

WESTAWAY, R., DEMIR, T., SEYREK, A. & BECK, A. 2006. Kinematics of active left-lateral faulting in southeast Turkey from offset Pleistocene river gorges; improved constraint on the rate and history of relative motion between the Turkish and Arabian plates. *Journal of Geological Society, London*, **163**, 149–164.